Shaker and Abbas Iraqi Journal of Science, 2023, Vol. 64, No. 5, pp: 2533-2544
DOI: 10.24996/ijs.2023.64.5.36

ISSN: 0067-2904

Material Recognition of Foreign Object Debris using Deep Learning

Dina Shaker*, Ayad Abbas
Department of Computer Science, University, of Technology, Baghdad, Iraq

Received: 24/3/2022 Accepted: 13/9/2022 Published: 30/5/2023

Abstract
Foreign Object Debris (FOD) is defined as one of the major problems in the airline maintenance industry, reducing the levels of safety. A foreign object which may result in causing serious damage to an airplane, including engine problems and personal safety risks. Therefore, it is critical to detect FOD in place to guarantee the safety of airplanes flying. FOD detection systems in the past lacked an effective method for automatic material recognition as well as high speed and accuracy in detecting materials. This paper proposes the FOD model using a variety of feature extraction approaches like Gray-level Co-occurrence Matrix (GLCM) and Linear Discriminant Analysis (LDA) to extract features and Deep Learning (DL) for classification. The data for this research was taken from the Shanghai Hongqiao International Airport runways. FOD has been done via utilizing a Convolutional Neural Network Classifier (CNN) with 27 layers. Those layers are distributed as follows: nine convolutional layers of type 1D; eight leaky ReLU layers; seven maxpooling 1D layers; two fully connected layers that are represented by the (Dense); and one flattening layer. The performance measures utilized in the system are precision, accuracy, F-score, and recall. The experimental results obtained after implementation and testing are of accuracy 99.8%, precision 100%, recall 100%, and F1-score is 100%. Experiments show that the proposed method has good performance in detection accuracy.

Keywords: Foreign Object Debris; Linear Discriminant Analysis; Gray-level co-occurrence matrix; Deep Learning; Convolutional Neural Network.

التعرف على مواد حطام الأجسام الغريبة باستعمال التعلم العميق

دينا رياض شاكر*, اياد روضان عباس
قسم علوم الحاسوب ، الجامعة التكنولوجية ، بغداد ، العراق

الخلاصة
تُعرَّف مشكلة حطام الأجسام الغريبة (FOD) بأنها إحدى المشكلات الرئيسية في صناعة صيانة الخطوط الجوية ، مما يقلل من مستويات السلامة. إنه يرمز إلى الجسم الغريب (FO) وهو جسم غريب قد يؤدي إلى إلحاق أضرار جسيمة بالطائرة ، بما في ذلك مشاكل المحرك ومخاطر السلامة الشخصية. لذلك ، من الأهمية اكتشاف التضاؤل من المستوى الأول في مكانه لضمان سلامة تحليق الطائرة. افتقرت أنظمة الكشف عن التضاؤل من المستوى الأول في الماضي إلى طريقة فعالة للتعرف التلقائي على المواد ، فضلاً عن السرعة العالية والدقة في الكشف عن المواد. يقترح هذا البحث نموذج التضاؤل من المستوى الأول

*Email: dina.r.shaker93@gmail.com

باستعمال مجموعة متنوعة من مناهج استخراج الميزات مثل مصفوفة التكرار ذات المستوى الرمادي (GLCM)
والتحليل التمييزي الخطي (LDA)
لاستخراج الميزات والتعلم العميق (DL) من أجل التصنيف. تم أخذ بيانات هذا البحث من مدارج مطار شنغهاي هونغكياو الدولي. تم إجراء التضاؤل من المستوى الأول من خلال استخدام مصنف الشبكات العصبية التلافيفي (CNN) مع 27 طبقة. مقاييس الأداء المستخدمة في النظام هي accuracy, precision ، recallو F1-score، النتائج التجريبية التي تم الحصول عليها بعد التنفيذ والاختبار كانت accuracy 99.8٪ و precision 100٪ وrecall 100٪ و F1-score 100٪ تظهر التجارب أن طريقتنا المقترحة لها أداء جيد في دقة الكشف. المعالجة المسبقة واستخراج الميزات والتصنيف هي مراحل النظام الثلاثة المقترحة.

1. Introduction

FOD on the runway has been widely known as one of the most serious challenges for airport safety since the Concord disaster at the Charles de Gaulle airport in France in 2000 [1]. FOD is a major issue in the aviation maintenance sector, lowering an aircraft's degree of safety. Actually, it might just be adequately minimized and controlled if the precise and right control approach is used. Between 1998 and 2008, the Aircraft Transport Safety Board (ATSB) received 116 FOD reports that affected high-capacity air transport aircraft. The majority of them occurred throughout the busiest hours of operations at major Australian airports. Nine of them took place on the apron of the aerodrome, whereas the remaining 12 took place on taxiways [2]. Metal pieces, debris, and other FOD on the airport runway are a danger to aircraft landing and taking off [3]. Considerable development was achieved in autonomous identification regarding airport pavement apparent disease and FOD via computers with the advancement of Image Processing and Deep Learning technologies [4]. The FOD Finder system, the Tarsier system, the FODetect system, and the iFerret system are currently the best FOD detection methods. A few of them are capable of obtaining the FOD image. However, they are unable to classify FOD automatically based on the FOD image [4].

Artificial intelligence and its sub-classes excel in a wide range of domains requiring smart decisions, from small binary classification assignments to huge clustering problems up to large recognition assignments [5]. Deep Learning technology has become a buzzword due to its ability to provide good results in the tasks of image classification, natural language processing (NLP), and object detection. This results from the availability of large datasets as well as powerful Graphics Processing Units (GPUs) [6]. The use of deep CNN is one of the most prominent approaches for image classification and object detection[7].

The proposed system combines two feature extraction methods, LDA and GLCM, for feature extraction and the number of layers in deep learning for classification.

The following is a breakdown of the paper structure: Section 2 introduces related works; Section 3 contains the proposed system; Section 4 introduces the results; and Section 5 is the conclusion.

Related work

Recently, some successful systems have been suggested to handle the FOD detection problem.

[8] provided a new FOD detection method that uses transfer learning and Deep Convolutional Neural Network (D-CNN) models. They created a FOD image dataset utilizing images of the airports and the research institute's headquarters at Shanghai Hongqiao Airport Terminal. The studies demonstrate that the suggested technique can boost material recognition accuracy by

39.6%. In this study, the performance of the three D-CNN models is compared. The first was AlexNet, which used MINC-trained parameters and had a 47% accuracy. The second was AlexNet, which used parameters from both the MINC and FOD datasets, a model with a 73%. The third model, with a 78%, was upgraded with parameters learned on the MINC and FOD datasets.

In[3], a recognition system dependent on You Only Look Once (YOLOv3) is provided. To detect small-scale FOD, this technique uses deep communication over a network for extracting features and multi-scale feature fusion. To test the strategy, sample datasets regarding FOD are created. Experiments demonstrated that the YOLOv3-based detection method accurately detects alien objects' detritus and is efficient and robust. FOD detection accuracy is 93.1%.

In[9], drones would be used to take photographs, and then a trained algorithm would be used to detect any FODs. The gathered image database supplied a wider range of images, enhancing the model's robustness. Two models were developed: one including six separate classes and the other a single object class model. The general online model and the local compact models were employed as training algorithms. The compact model can analyze images quickly, but it loses the general accuracy of the model. Furthermore, the general model has a higher precision compared to the small model. FOD detection accuracy for a single class is 88.8% and for multiclass is 96.3%.

In[6], a Deep Learning technique for FOD classification is provided. The Convolutional Neural Network (CNN) is a Deep Learning technique that produces substantial results in image recognition. The study's goal is to establish the CNN algorithm model with the highest classification accuracy for FODs. CNNs are multilayer neural networks with a supervised learning architecture. They are composed of two components: feature reviewers and trainable classifiers. The research began with creating a dataset and a CNN algorithm model, followed by the addition of training and testing data. The CNN model uses a 64×64 input image, a learning rate of 0.001, a filter size of 3 x 3, the epochs are 100, the training data is 1200 data points, and the test data is 20. A single layer of convolution is utilized. The algorithm developed can classify FOD objects into six categories with an accuracy of 86.6% and provide the best classification results into four categories with an accuracy of up to 90%.

2. The Proposed System

The FOD dataset is divided into three classes, each having a total of 3000 images. 70% of samples have been chosen at random for training and 30% for testing. The samples were then preprocessed. The FOD offers a classification model that combines LDA and GLCM to extract FOD features and deep learning to extract powerful features and classify the FOD. Figure 1 shows the block diagram of the proposed system.

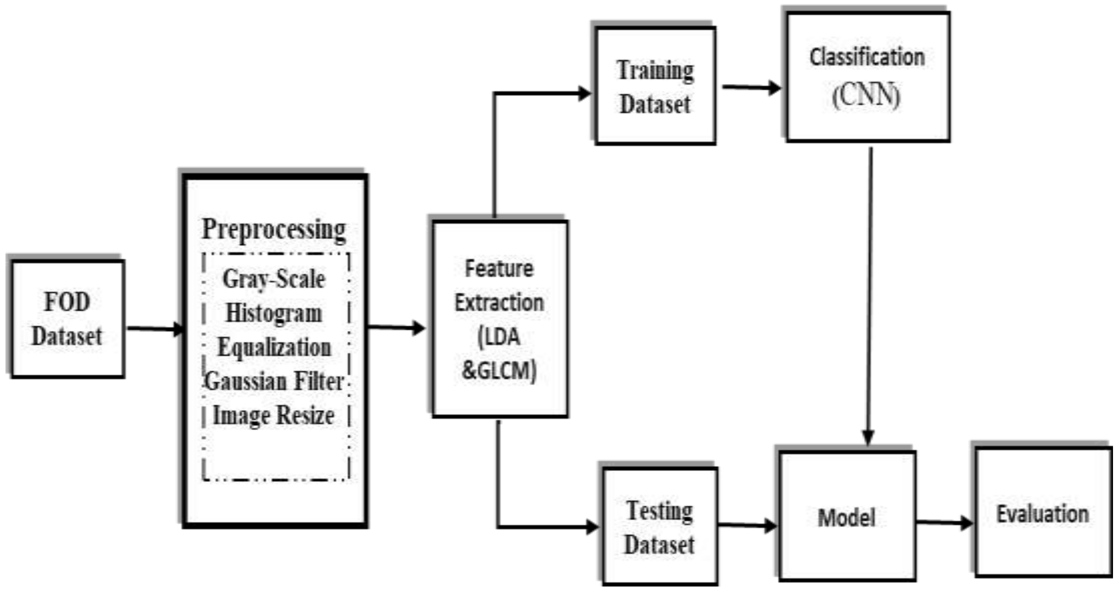

Figure 1: The block diagram of the proposed system.

3.1 Dataset Description

The image dataset that has been used in this paper was collected from the runways of Shanghai Hongqiao International Airport [10]. In this dataset, three common FOD materials are used: metal, plastic, and concrete. The most common locations for these materials are runways and taxiways. Under bright light in an outdoor context, extreme reflectance phenomena can occur in metal and plastic. To complicate matters further, these images were captured on concrete runways or taxiways. The concrete background of metal or plastic images makes separating these two materials from the background extremely difficult. As a result, careful handling is required to identify metal, plastic, and concrete appropriately.

The FOD dataset has three aspects. First, each material category had a large amount of intra-class diversity. The shapes or identities of images belonging to the same material group were frequently radically different. Second, the background of all of the images was concrete. Third, the images were taken in naturalistic contexts. Therefore, this dataset is more complicated. There are three classes in the FOD dataset, totaling 3000 pictures: 1000 pictures of metal, 1000 pictures of concrete, and 1000 pictures of plastic. Randomly select 70% of samples for training and 30% for testing in the FOD dataset. The statistics of the FOD dataset have been listed in Table 1.

Table 1: Characteristics of the FOD dataset

Object	*Training*	*Testing*
Metal	700	300
Plastic	700	300
Concrete	700	300

The FOD image dataset samples can be shown in Figure 2.

(a) (b) (c)

Figure 2: The FOD dataset image samples that range as a. Concrete FOD, b. Metal FOD, c. Plastic FOD

3.2 FOD Image Preprocessing and Feature Extraction

3.2.1 FOD Image Preprocessing

The primary purpose of preprocessing is to enhance image data by removing undesired distortions or boosting certain image attributes that are required for future processing.

A. Grayscale Image

Grayscale images have one dimension (channel) and consist of only gray shades of colors, which are only 256 gray colors when 8-bit representation is used. These image combinations are referred to as monochrome since monochrome refers to the presence of only one color, while color refers to chromium. The conversion of the image from RGB mode to grey is accomplished using Eq. (1).

$$Gray = (0.21 \text{ xR}) + (0.72 \text{ xG}) + (0.07 \text{ xB}) \quad (1)$$

Where, R: red, B: blue and G: green.

The reason for this conversion is to reduce the amount of data required to represent the image. Images in the grayscale color space have only one channel, whereas images in the RGB (Red, Green, and Blue) color space require three channels to be saved and represented in the machine as a digital image. The translation of colored images to grayscale increases processing speed. Naturally, the grayscale image has an intensity that is stored as an 8-bit integer, giving 256 distinct grayscale possibilities ranging from white to black.

B. Histogram Equalization

Histogram equalization can be defined as a spatial domain approach that generates an output image with an even distribution of the pixel intensities. This indicates the fact that the histogram of the output image has been flattened and extended in a systematic manner [11]. Due to its simple function and efficacy, histogram equalization is commonly utilized for contrast enhancement in several applications [12]. Histogram equalization can be shown by Eq. (2).

$$\mathrm{Cdf}\,(\mathrm{K}) = \sum_{\mathrm{i}=1}^{\mathrm{K}} \mathrm{r(i)} \tag{2}$$

Where, K represents the gray value and r illustrates the image histogram.

$$\mathrm{F[pixel]} = \mathrm{round}\left(\left(\frac{\mathrm{cdf(K)} - \mathrm{cdf(K)_{min}}}{\mathrm{N*M} - \mathrm{cdf(K)_{min}}}\right) * (\mathrm{G} - 1)\right)$$

(3) Where, $\mathrm{cdf(K)_{min}}$: represents the minimal value of cumulative distribution function.
$N * M$: Columns and rows number of images.
G: Gray levels used =256.

C. Gaussian Filter

This filter uses a Gaussian function in order to eliminate image noise. Because the Laplacian operator is sensitive to the noise that can obstruct its efficiency, it is necessary to reduce noise. The Gaussian function generates a filter which could be implemented on every one of the image pixels. It is estimated in 2 dimensions via Eq. (4):

$$GF(\alpha,\beta) = \frac{1}{(2\pi\sigma^2)} e^{-\frac{(\alpha^2+\beta^2)}{2\sigma^2}}$$

Where, α represents the measure between the origin point and the horizontal axis, and β represents the measure between the origin point and the vertical axis. σ represents the Gaussian distribution's standard deviation [13]. Thus, the Difference of Gaussian (DoG) is one of the common approximations to the Laplace of Gaussian (LoG) operator, and those are highly significant basic image transformations [16].

D. Image Resize

Image resizing is a technique used in image processing to enlarge and shrink the size of a given image in pixel format. The objective of image resizing is to reduce the amount of data, which reduces processing time. Changing the FOD image dimensions is an important stage where the images are resized based on a bilinear interpolation routine. The image size is changed to 50 * 50 pixels, making all images of one size and allowing a faster training process.

3.2.2 FOD Feature Extraction

Feature extraction extracts the best discriminating features of the image that are not susceptible to unpredictable environmental differences such as contrasts in scale, illumination, and pose. In this study, two approaches to feature extraction have been utilized: LDA and GLCM.

A. Linear Discriminant Analysis (LDA)

LDA is a data transformation method that takes a set of data and turns it into new data with specific statistical qualities [15]. For dimensionality reduction, LDA is a prominent supervised method. In the pattern recognition and computer vision communities, the LDA is a traditional statistical approach that reduces dimensionality while retaining as much class-discriminating information as possible. LDA works on the assumption that all data is available beforehand, and LDA feature space is calculated via determining the eigen decomposition of a suitable matrix. In some cases, the data is provided in a sequential order, and LDA features must be incrementally updated through the observation of new incoming samples [16]. The LDA method's conventional implementation necessitates the availability of all samples in advance. The LDA approach finds an orientation which decreases the high-dimensional feature vectors that belong to various classes to a lower-dimensional feature space such that projected feature vectors of one of the classes in such a lower-dimensional space have been well separated from other classes' feature vectors [17], as shown in Eq. (5) to (8) below:

$$\mu_j = \frac{1}{n_j} \sum_{x_i \in \omega_j} x_i \tag{5}$$

$$\mu = \frac{1}{N} \sum_{i=1}^{N} x_i = \sum_{i=1}^{c} \frac{n_i}{N} \mu_i \tag{6}$$

$$S_B = \sum_{i=1}^{c} n_i (\mu_i - \mu)(\mu_i - \mu)^T \tag{7}$$

$$S_W = \sum_{j=1}^{c} \sum_{i=1}^{n_j} (x_{ij} - \mu_j)(x_{ij} - \mu_{j)})^T \tag{8}$$

Where, Xin represents the i^{-th} sample in j the class.

$$W = S_W^{-1} S_B \tag{9}$$

$$Y = XV_K \tag{10}$$

Where, N: The total number of samples; n_i represents number of samples of i^{-th} class; μ_i represents projection of mean of i^{-th}; µ Projection of the total average value of all classes; S_B inter-class variance; and S_{wi} the within-class variance of i^{-th} class; represents difference between mean.

B. Gray-level co-occurrence matrix (GLCM)

The statistical distributions of intensity value combinations at distinct positions in relation to one another in the image are used for extracting 2nd order statistical texture features. Statistics have been classified as 1st, 2nd, or higher order according to the number of points of intensity in the image. Higher-order statistics are theoretically possible, but because of computational complexity, they cannot be implemented. Texture features store information on the structural arrangement of the surfaces as well as their relations with their surroundings. From correlation, energy, Inverse Difference Moment (IDM), entropy, summation variance, homogeneity, contrast, autocorrelation, dissimilarity, IDM normalized, maximum probability, and many more texture-based properties are derived. Some of them have been formulated as follows [18]:

a. Energy: which is another name for the 'uniformity' or the 'angular second moment'. It results in the summation of the square elements in the GLCM matrix. It's by mean values of the homogeneous areas to the non-homogeneous ones. It is high in the case where the frequency of the high repeated image pixel is high, as shown in Eq. (11):

$$\text{Energy} = \sum_{n,m=0}^{k-1} (P_{nm})^2 \tag{11}$$

b. Entropy: which is the calculation of image randomness. As a result, the homogeneous image will lead to lower values of entropy, as shown in Eq. (12):

$$Entropy = \sum_{n,m=0}^{k-1} -ln(P_{nm}) P_{nm} \tag{12}$$

c. Contrast: which is a measure of intensity, linking contrast between a pixel and its neighbor in the whole image, as shown in Eq. (13):

$$Contrast = \sum_{n,m=0}^{k-1} P_{nm} (n-m)^2 \tag{13}$$

d. Correlation: which measures the linear dependencies of the gray tones in the image. It is a specification of the way that a pixel is related to its neighbors, as shown in Eq. (14):

$$Correlation = \sum_{n,m=0}^{k-1} P_{nm} \frac{(n-\mu)(m-\mu)}{\sigma^2} \quad (14)$$

e. Homogeneity: It refers to the similarity of the pixels. The GLCM of the homogeneous image provides its value as 1. Its value is very small in the case where the image texture requires minimal alterations, as shown in Eq. (15):

$$Homogeneity = \sum_{n,m=0}^{k-1} \frac{P_{nm}}{1+(n-m)^2} \quad (15)$$

Where, P_{nm}= (n, m) th element of normalized GLCM.
μ = average of the GLCM that has been estimated using the Eq. (16):

$$\mu=\sum_{n,m=0}^{k-1} nP_{nm} \quad (16)$$

Where, σ = the variance of the intensity values of all of the pixels that have been calculated with the use of:

$$\sigma^2 = \sum_{n,m=0}^{k-1} P_{nm}(n-\mu)^2 \quad (17)$$

Where, K= number of the gray level values in the image.

In this paper, the proposed method combines LDA and GLCM features for image classification. Two features are extracted by the LDA and six features by the GLCM, then they are combined to have eight features that will be used for classification.

3.2.3 FOD Classification with Convolutional Neural Network

Deep learning adds more "depth" (difficulty) to the model and changes the data with a variety of functions that allow data to be represented in a hierarchical way, with many layers. People who study DL use more complicated models that can do a lot of work at the same time. This means that DL can solve more difficult problems very quickly and very well. DL is made up of a variety of distinct components, depending on the network architecture used (e.g., convolutions, pooling layers, fully connected layers, gates, memory cells, activation functions, encode/decode schemes, and so on) [19]. The learning skills of neuronal cells associated by synapses in the human brain serve as inspiration for artificial neural networks. ANNs are unsuitable for image classification because these networks result in image size overfitting. CNNs are typically employed for image recognition jobs. The CNNs are the most prevalent [20]. Convolutional neural networks are one of the main categories for doing image recognition. It takes an input image, processes it, and classifies it under certain categories. A free open-source deep learning library, Keras, was used to implement the CNN model. Each input image will pass through a series of convolution layers with filters (Kernals), pooling, and fully connected layers (FC) to classify an object with probabilistic values between 0 and 1. The CNNs work the same way whether they have 1, 2, or 3 dimensions. The difference is the structure of the input data and how the filter, also known as a convolution kernel or feature detector, moves across the data [21].

The suggested CNN model will be described in-depth and illustrated in Figure 3, which will demonstrate the 27 layers that make up the model as in the following:

1. Nine convolutional layers for feature extraction of type 1D.
2. Eight Leaky ReLU layers.
3. Seven Maxpooling 1D layers.
4. Two fully connected layers that are represented by the (Dense).
5. One flattened layer.

The CNN model begins with convolutional layers (Conv1D) with a filter range (16, 32, 64, 128, 256, 512, 1024, 50) and the kernel size is 3, stride =1. Then, leaky ReLU layers with an alpha value of 0.3 are used to reduce the high negative values that affect the results and bring them closer to zero. Then, Maxpooling 1D layers with pooling size=1, stride=1. And Dense layers with activation=linear to make the system work for classification and regression. Finally, flattens the layer to arrange the number of features in one line evenly. The learning rate that has been used is lr=0.0001. These layers are applied to the training dataset and tested by generating 3,304,293 parameters. The CNN layer can be shown in figure 3.

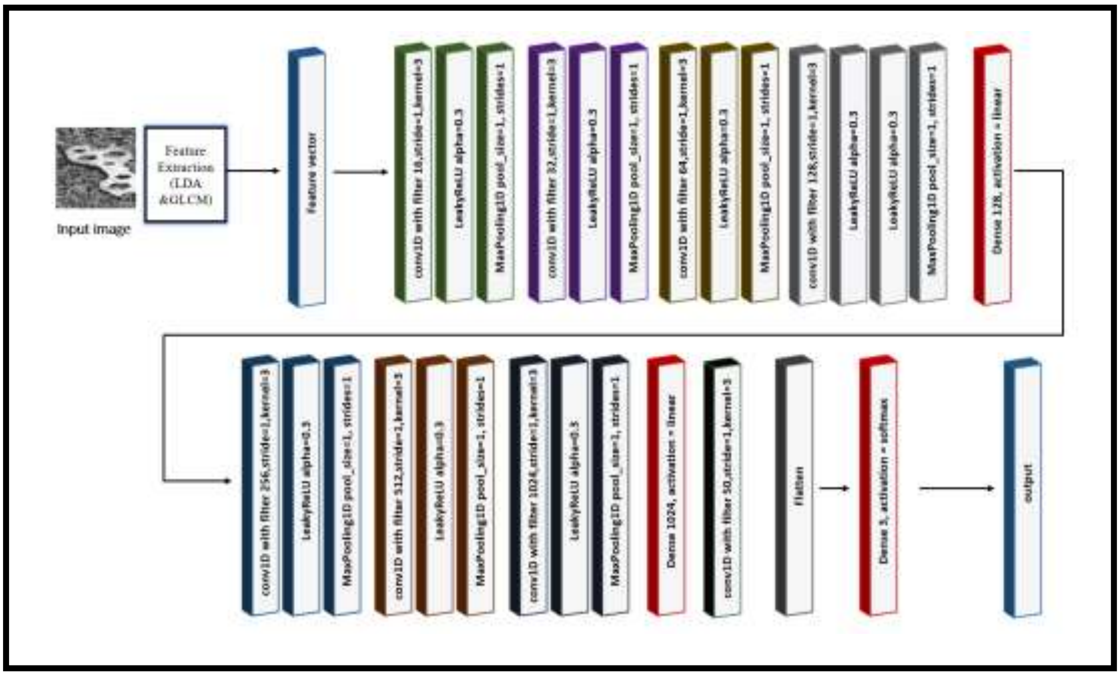

Figure 3: The structure of the CNN layers.

4. Results

There are various metrics of evaluation by which many classifiers can be examined and analyzed. To measure the performance of all models, we employ the most standard performance measures, which are precision, recall, and F-score metrics, as shown in the following equations [22].

4.1. Accuracy:

Represents the most significant one of the metrics for evaluating the classification. It’s the proportion of correct predictions, and the equation is used to determine it.

$$\text{Accuracy} = \frac{\text{TP+TN}}{\text{TP+TN+FP+FN}} \tag{18}$$

4.2. Precision**:**

This is often known as the positive predictive value, and is calculated as the ratio of positive measurements among all positive cases obtained from the model.

$$\text{Precision} = \frac{\text{TP}}{\text{FP+TP}} \tag{19}$$

4.3. Recall:

It represents the portion of the instances which have been predicted accurately as positive to actual attack class size, and it is computed with the use of an equation.

$$\text{Rrcall} = \frac{\text{TP}}{\text{FN+TP}} \tag{20}$$

4.4. F1-score**:**
This is the geometric average value of the precision and recall, also known as the F measure.

$$\mathrm{F1-score} = \frac{2*Precision*Recall}{Precision+Recall} \tag{21}$$

In which TP (True Positive) represents the number of the samples that have been correctly assigned to a class; and TN (True Negative) represents the number of the samples that do not belong to a class and were not classified to that class; the number of samples belonging to one class yet incorrectly classified into another is referred to as FN (False Negative); the number of samples incorrectly classified into a specific class yet not belonging to that class is referred to as FP (False Positive) [23].

Figure 4 shows the result of the CNN classifier. The strategy of mixed features, which combines the LDA and GLCM features, gives the best result because it still retains its satiability and gives only the important features, so when used with the CNN, it gives more accuracy and power in classification. CNN was shown to be effective in FOD classification with 27 layers. For example, the accuracy is 99.8%, precision is 100%, recall is 100%, and F1-score is 100%.

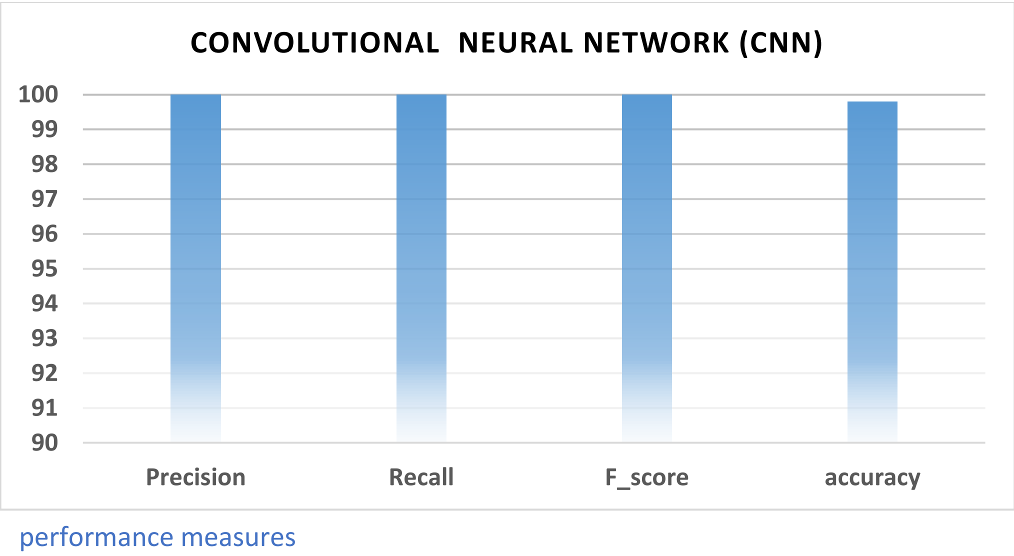

Figure 4: The result of the CNN classifier

5. Conclusion

Recognizing FOD materials is a difficult but necessary task which should be done in order to keep airports safe. Separating objects from the backdrop is exceedingly difficult due to the concrete background. This research proposes a new FOD classification system that combines the GLCM and LDA features. After reprocessing the image dataset, features are extracted using a combination of two feature extraction approaches. Lastly, CNN is utilized for classification, with a 99.8% accuracy rate. The experimental results using FOD datasets demonstrate that the proposed method is effective.

This method has the benefit of being able to instantly distinguish FOD items acquired by the camera. This method's shortcoming is the intricacy of CNN layers and the technique for feature extraction. For future work, deep learning will be used for feature extraction and machine learning for classification.

References

[1] N. Yonemoto, A. Kohmura, S. Futatsumori, K. Morioka, and N. Kanada, "Two Dimensional Radar Imaging Algorithm of Bistatic Millimeter Wave Radar for FOD Detection on Runways," *MWP 2018 - 2018 Int. Top. Meet. Microw. Photonics*, pp. 1–4, 2018, doi: 10.1109/MWP.2018.8552847.

[2] R. Hussin, N. Ismail, and S. Mustapa, "A study of foreign object damage (FOD) and prevention method at the airport and aircraft maintenance area," *IOP Conf. Ser. Mater. Sci. Eng.*, vol. 152, no. 1, 2016, doi: 10.1088/1757-899X/152/1/012038.

[3] P. Li and H. Li, "Research on FOD Detection for Airport Runway based on YOLOv3," *Chinese Control Conf. CCC*, vol. 2020-July, pp. 7096–7099, 2020, doi: 10.23919/CCC50068. 2020.9188724.

[4] W. Guo, H. Fang, and N. Wang, "New Method of Airport Pavement Health Inspection Based on MobileNet-SSD and Mask R-CNN," *J. Phys. Conf. Ser.*, vol. 1885, no. 2, 2021, doi: 10.1088/ 1742-6596/1885/2/022048.

[5] H. A. R. Akkar, A. H. Wael, and I. H. M. Al-dosari, "PSO Trained Hybrid Intelligent Classifier Using Wavelet and Statistical Features for Pipeline Leak Classification," *Iraqi J. Comput. Commun. Control Syst. Eng.*, pp. 1–9, 2019, doi: 10.33103/uot.ijccce.19.1.1.

[6] K. Adi, C. E. D. I. Widodo, A. P. Widodo, and U. S. R. I. Margiati, "DETECTION OF FOREIGN OBJECT DEBRIS (FOD) USING CONVOLUTIONAL NEURAL NETWORK (CNN)," *J. Theor. Appl. Inf. Technol.*, vol. 100, no. 1, pp. 184–191, 2022.

[7] M. M. Mahmoud and A. R. Nasser, "Dual Architecture Deep Learning Based Object Detection System for Autonomous Driving," *Iraqi J. Comput. Commun. Control Syst. Eng*, vol. 21, no. 2, pp. 36–43, 2021.

[8] H. Xu, Z. Han, S. Feng, H. Zhou, and Y. Fang, "Foreign object debris material recognition based on convolutional neural networks," *Eurasip J. Image Video Process.*, vol. 2018, no. 1, pp. 0–9, 2018, doi: 10.1186/s13640-018-0261-2.

[9] L. Felipe, F. Gonzalez, and P. Trotter, "Live Detection of Foreign Object Debris on Runways Detection using Drones and AI," *Proc. ofthe 2022 IEEE Int. Aerosp. Conf. Inst. Electr. Electron. Eng. Inc.. (In Press.*, no. 2021, pp. 1–14, 2022.

[10] "data.7z-Google Drive." https://drive.google.com/file/d/1UTxZQUipkX6_r C9AoCaweeee OPrOG1_ B/edit (accessed Apr. 29, 2022).

[11] R. P. Singh and M. Dixit, "Histogram Equalization: A Strong Technique for Image Enhancement," *Int. J. Signal Process. Image Process. Pattern Recognit.*, vol. 8, no. 8, pp. 345–352, 2015, doi: 10.14257/ijsip.2015.8.8.35.

[12] V. P. Vishwakarma, S. Pandey, and M. N. Gupta, "Adaptive histogram equalization and logarithm transform with rescaled low frequency DCT coefficients for illumination normalization," *Int. J. Recent Trends Eng. Technol.*, vol. 1, no. 1, pp. 318–322, 2009.

[13] L. Mary, "International Conference on Computational Intelligence and Data Science, ICCIDS 2019," *Procedia Comput. Sci.*, vol. 167, no. February, 2020.

[14] A. A. Karim and R. Sameer, "Improvement of Harris Algorithm Based on Gaussian Scale Space," *Eng. Technol. J.*, vol. 37, no. 1B, pp. 1–5, 2019, doi: 10.30684/etj.37.1b.1.

[15] A. R. Abbas and A. R. Kareem, "Age estimation using support vector machine," *Iraqi J. Sci.*, vol. 59, no. 3, pp. 1746–1756, 2018, doi: 10.24996/IJS.2018.59.3C.19.

[16] Y. Aliyari Ghassabeh, F. Rudzicz, and H. A. Moghaddam, "Fast incremental LDA feature extraction," *Pattern Recognit.*, vol. 48, no. 6, pp. 1999–2012, 2015, doi: 10.1016/j.patcog. 2014.12.012.

[17] J. Li, B. Zhao, and H. Zhang, "Face recognition based on PCA and LDA combination feature extraction," *2009 1st Int. Conf. Inf. Sci. Eng. ICISE 2009*, no. 20042013, pp. 1240–1243, 2009, doi: 10.1109/ICISE.2009.581.

[18] Priyanka and D. Kumar, "Feature Extraction and Selection of kidney Ultrasound Images Using GLCM and PCA," *Procedia Comput. Sci.*, vol. 167, no. 2019, pp. 1722–1731, 2020, doi: 10.1016/j.procs.2020.03.382.

[19] A. Kamilaris and F. X. Prenafeta-Boldú, "Deep learning in agriculture: A survey," *Comput. Electron. Agric.*, vol. 147, pp. 70–90, 2018, doi: 10.1016/j.compag.2018.02.016.

[20] R. M. J. Al-Akkam and M. S. M. Altaei, "Plants Leaf Diseases Detection Using Deep Learning," *Iraqi J. Sci.*, vol. 63, no. 2, pp. 801–816, 2022, doi: 10.24996/ijs.2022.63.2.34.

[21] S. Kiranyaz, O. Avci, O. Abdeljaber, T. Ince, M. Gabbouj, and D. J. Inman, "1D convolutional neural networks and applications: A survey," *Mech. Syst. Signal Process.*, vol. 151, no. May, 2021, doi: 10.1016/j.ymssp.2020.107398.

[22] S. Khan, E. Sivaraman, and P. B. Honnavalli, "Performance evaluation of advanced machine learning algorithms for network intrusion detection system," *Lect. Notes Networks Syst.*, vol. 116, no. January 2020, pp. 51–59, 2020, doi: 10.1007/978-981-15-3020-3_6.

[23] H. A. Jaber and M. T. Rashid, "HD-sEMG Gestures Recognition by SVM Classifier for Controlling Prosthesis," *Iraqi J. Comput. Commun. Control Syst. Eng.*, pp. 10–19, 2019, doi: 10.33103/uot.ijccce.19.1.2.